High-Frequency Characteristics of Overhead Multiconductor Power Lines for Broadband Communications

Pouyan Amirshahi, *Student Member, IEEE*, and Mohsen Kavehrad, *Fellow, IEEE*

Abstract—This paper presents a channel model suitable for multiwire overhead medium voltage lines. This model, incorporating ground admittance, is more appropriate at higher frequencies than predicted by Carson's model of 1926. The proposed model is further used to evaluate the multipath channel impulse response and associated capacity limit in sample power distribution grids for applications in broadband over power lines communications. For a sample grid model, comparison is made to the capacity value predicted based on the Carson's model, and it is demonstrated that the older model underestimates the potential of the overhead lines for broadband transmissions, significantly.

Index Terms—Capacity, channel model, ground admittance, impulse response, medium voltage, power line communications.

I. INTRODUCTION

THE medium-voltage power grid, typically carrying megawatts of power at 11 000 V, reaches within a few hundred meters of most dwellings within the industrialized world. The same grid is a potentially excellent communications medium, offering bandwidths well beyond 100 MHz and potentially more, with Shannon capacity values well into the gigabit range. This fact was highlighted very recently by the authors, in conference paper [1].

Fast Internet access is growing from a convenience into a necessity in all aspects of our daily lives. Unfortunately, this has been held back by the high expenses of wiring infrastructure essential to deliver such high-speed Internet access especially to private homes, small offices and rural areas, where the installation of any kind of new wires tilts the scales of the economic feasibility to a nonprofitable state. This problem is known as the "last mile problem" which has been an active area of research in recent years.

The lines in a power delivery network may be characterized by a number of criteria. For example, by line voltages including: high voltage (HV), medium voltage (MV), and low voltage (LV) or within a distribution grid, in the form of either overhead (OH) or underground (UG) cable topologies.

The power distribution grid resembles an omnipresent, widely branched hierarchical structure. Therefore, the structure of MV and LV power distribution grid is appropriate for Internet access, offering both last mile and last meter solutions. In Europe, there have been significant efforts to utilize the LV distribution grid consisting mostly of shielded underground cables and in-building LV network as a medium for broadband service delivery, [2]–[8]. Unlike the European system, a typical power line access network in the U.S. is composed of MV distribution grid and LV lines to and from houses. It is usually composed of three phases and a neutral wire or three phases and a grounded neutral wire. Measurements over three-phase overhead MV lines were performed in South Korea [9], [10]. Currently, many vendors have proposed use of frequencies between 2–50 MHz for broadband over power lines (BoPL) application [11].

Overhead MV lines differ considerable in structure and physical properties compared with other wire-lines as twisted-pair, coaxial, and fiber-optic cables. The power lines in the U.S. hang overhead at a height of ~10 m above ground, for more than 85% of locations, simply because over ground wiring is ten times cheaper than underground. Typically, four wires, three phases and a neutral (sometimes a grounded neutral) with ~0.5 to 1 m spacing between wires are used above ground. Wires are made of aluminum with 70% of standard annealed copper conductivity.

Originally designed for power delivery rather than signal transmission, power line has many nonideal properties as a communications medium. Impedance mismatches at joints cause reflections that generate conditions similar to those created by multipath fading in wireless communications. While there have been significant research efforts to characterize European ground cables, a proper theoretical model for multiconductor overhead MV lines, a typical situation in the U.S., was not available, until the recent work by the authors [1] that suggests the MV grid is a potentially excellent communications medium, offering bandwidths well beyond 100 MHz and potentially many gigahertz, with Shannon capacities well into the gigabit range. The high bandwidth and the ubiquitous nature of the MV grid make it a communication engineer's gold mine, whose potential has hardly been exploited.

As an extension of the work by D'Amore *et al.* [12], in this paper, a channel model is presented suitable for multiconductor overhead MV lines. The suggested model, accounting for ground admittance, is more appropriate at higher frequencies than what was predicted by the Carson's model [13]. More can be found on communications over multiconductor transmission lines (MTL), involving more than two conductors, in

references [20], [30], and [31]. The proposed model is further utilized to evaluate the channel impulse response and transmission capacity in some sample power distribution networks. Our channel modeling belongs to the category of bottom-up approaches, and is different from the traditional top-down multipath-based approaches. This kind of approach allows for the *a priori* computation of the transfer function (whereas a top-down one does not) at the expense of a detailed knowledge of topology, cable properties, and terminating impedances.

In Section II, a review of existing models is provided. In Section III, mathematical derivations of the proposed model are presented. Section IV presents a new communications channel model suitable for these lines. In Section V, numerical performance results are provided. Concluding remarks and references end the discussions.

II. REVIEW OF EXISTING RESEARCH EFFORTS

A. Single Conductor Over High-Loss Earth

Historically, finding the propagation constant of "a thin wire over earth" has been of interest to researchers since early 20th century because of its application in power transmission and telephone communications. These systems operate at very low frequencies. At these frequencies, height of wire is a small fraction of wavelength and all the coupled energy into the wire propagates in quasi-transverse-electromagnetic (TEM) modes. Thus, the early works in this field focused on finding the distribution characteristics of this type of propagation mode in transmission lines.

Carson reported the earliest solution for this problem in 1926 [13]. In his work, he calculated values for distribution parameters of a quasi-TEM mode in a transmission line. In doing so, he made some assumptions. He first assumed that the displacement current on the earth surface is negligible; therefore, the effect of earth conductivity on the *per-unit-length* shunt admittance can be neglected. Moreover, he assumed that propagation constant in the air is not significantly different than that in a dielectric, thus, he used Laplace's equation for two-dimensional wave equation in air. These assumptions restrict the solution to very low frequencies and/or perfectly conducting earth.

To find the exact solution for this problem at high frequencies with higher loss ground return, we need to derive modal equations. Kikuchi [14], [15] in 1956 derived exact modal equations for very thin overhead wires. In his works, Kikuchi used quasi-static and asymptotic expansion of the exact modal equation to investigate the transition from quasi-TEM to surface wave propagation. Carson's method is essentially a low-frequency approximation of transmission line mode. On the contrary, Kikuchi's result is associated with the entire frequency spectrum of the same mode. Kikuchi showed, experimentally and theoretically, that as frequency increases, the transmission line quasi-TEM mode reverts to a transverse-magnetic (TM) mode. According to Kikuchi, as frequency increases there exist a high field concentration around the wire and large longitudinal displacement currents that act as return currents over the air, thus minimizing the role of earth as a return current path. Therefore, beyond certain frequency, the path loss of transmission line diminishes by an increase in frequency. In 1972, Wait [16], [17] extended Kikuchi's

work and solved the exact modal equation for a thin overhead wire, numerically.

Basically, for analyzing this problem, we need to satisfy boundary conditions on the interface between the surface of wire and the medium surrounding the wire. Suppose a wire with thickness a is positioned at a height $z = h$ above the surface of the earth parallel to horizontal x axis. Permittivity, permeability, and conductivity of ground are, respectively, represented by ε_g, μ_g, and σ_g. These parameters for wire are expressed by ε_w, μ_w, and σ_w. Parameters ε_0 and μ_0 are permittivity and permeability of the free space. The electric current propagates along x-direction in this wire with a propagation constant γ. For boundary conditions, we will have

$$E_x(x,h,a)|_{\text{wire}} = E_x(x,h,a)|_{\text{air}}. \tag{1}$$

The x-component of the electric field on the wire is expressed by

$$E_x(x,h,a)|_{\text{wire}} = z_i'(\gamma)I(x) \tag{2}$$

where $z_i'(\gamma)$ is the wire inner impedance expressed as

$$z_i'(\gamma) = \frac{\omega\mu_w u_w I_0(ju_w a)}{2\pi a k_w^2 I_1(ju_w a)} \tag{3}$$

$$k_w = k_0\sqrt{\frac{\varepsilon_w}{\varepsilon_0} - \frac{j\sigma_w}{\omega\varepsilon_0}} \quad k_o = \omega\sqrt{\mu_0\varepsilon_0}$$

$$u_w = \sqrt{k_w^2 - \gamma^2}. \tag{4}$$

Following the procedure in [18], the x-component of electric field in the air is obtained by:

$$E_X(x,h,a)|_{\text{air}} = \frac{-j\omega\mu_0}{\pi}M(\gamma,h,a)I(x) \tag{5}$$

$$M(\gamma,h,a) = \frac{k_0^2 - \gamma^2}{2k_0^2}\Lambda(\gamma,h,a) + S_{1g}(\gamma,h,a)$$

$$- \frac{\gamma^2}{k_0^2}S_{2g}(\gamma,h,a) \tag{6}$$

$$S_{1g}(\gamma,h,a) = \frac{1}{2}\int_{-\infty}^{\infty}\frac{\exp(-u_0 2h)}{u_0 + u_g}\exp(-jz\lambda)d\lambda \tag{7}$$

$$S_{2g}(\gamma,h,a) = \frac{1}{2}\int_{-\infty}^{\infty}\frac{\exp(-u_0 2h)}{k_g^2 k_0^{-2}u_0 + u_g}\exp(-jz\lambda)d\lambda \tag{8}$$

$$\Lambda(\gamma,h,a) = K_0\left(ja\sqrt{k_0^2 - \gamma^2}\right)$$

$$- K_0\left(j\sqrt{4h^2 + a^2}\sqrt{k_0^2 + \gamma^2}\right) \tag{9}$$

$$u_0 = \sqrt{\lambda^2 + \gamma^2 - k_0^2} \tag{10}$$

$$u_g = \sqrt{\lambda^2 + \gamma^2 - k_g^2} \tag{11}$$

where K_0 is the modified Bessel function of second kind order zero. S_{1g} and S_{2g} are called Sommerfeld integrals.

By the help of (3)–(11), (2) can be solved for γ. Equation (2) is composed of Bessel and Sommerfeld integrals that are functions of γ; therefore, the general explicit answer to (2) cannot be obtained and it needs numerical methods to solve (2) for propagation constant γ. Solving this equation numerically is not an easy task, as there is no certainty about starting point for γ. An unsuitable starting point can cause the answers to diverge. D'Amore *et al.* in [12] assumed $k_w \gg k_0$ and $k_0^2 - y^2 \approx 0$, which are admissible for the cases when wavelength is a small fraction of the height of wire above ground. For example, for a wire system with 10 m height above the terrain, these estimates are valid, approximately up to 100 MHz frequencies. With these assumptions in mind, the propagation constant can be expressed as

$$\gamma^2 = k_0^2 \left[\frac{2\pi z_i'(j\omega\mu_0)^{-1} + \ln\left(\frac{2h}{a}\right) + 2\hat{S}_{1g}(h)}{\ln\left(\frac{2h}{a}\right) + \hat{S}_{2g}(h)} \right] \quad (12)$$

$$z_i' = \frac{\omega\mu_w I_0(jk_w a)}{2\pi a k_w I_1(jk_w a)} \quad (13)$$

$$\hat{S}_{1g}(h) = 0.5\ln(1 + \alpha'r^{-1}) \quad (14)$$

$$\hat{S}_{2g}(h) = \frac{k_0^2}{k_g^2 + k_0^2}\ln(1 + \beta'r^{-1}) \quad (15)$$

$$\alpha' = \frac{2}{\sqrt{k_0^2 - k_g^2}} \text{ and } \beta' = \frac{k_0^2 + k_g^2}{k_0^2\sqrt{k_0^2 - k_g^2}} \quad (16)$$

$$r = \sqrt{4h^2 + a^2}. \quad (17)$$

Carson in [13] assumed $|a\sqrt{k_0^2 - \gamma^2}| \ll 1$, $|2h\sqrt{k_0^2 - \gamma^2}| \ll 1$, $2h \gg a$, $|k_0h| \ll 1$, and $|k_0/k_g| \ll 1$. With these approximations, the propagation constant is equal to

$$\gamma = k_0\sqrt{1 - \frac{J_c}{\ln\left(\frac{2h}{a}\right)}} \quad (18)$$

where J_c is given by

$$J_c = \frac{2}{k_g^2} \int_0^\infty \left(\sqrt{\lambda^2 - k_g^2} - \lambda\right) e^{-2\lambda h} d\lambda. \quad (19)$$

Carson's integral in (19) can be expressed as a series. Unfortunately, even with these assumptions and using the series expansion, solution appears to be rather complicated. However, Carson noted that the leading terms in the series are of importance in many practical cases, and use of these terms leads to a simple closed form answer [13].

For a better understanding of these expressions, Fig. 1 shows the real and imaginary parts of the propagation constant of a wire above the ground surface, evaluated by three different methods. This wire is characterized by $\sigma_w = 3.8 \times 10^7$ S/m and $\varepsilon_w = 2.3 \times 10^3\varepsilon_0$ and is positioned at 10 m above the earth. The wire has a radius of 1 cm. Earth is characterized by $\sigma_g = 0.005$ S/m and $\varepsilon_g = 13\varepsilon_0$. As it is shown in this figure, in terms of attenuation constant, the three formulations agree at low frequencies and increase with frequency increments,
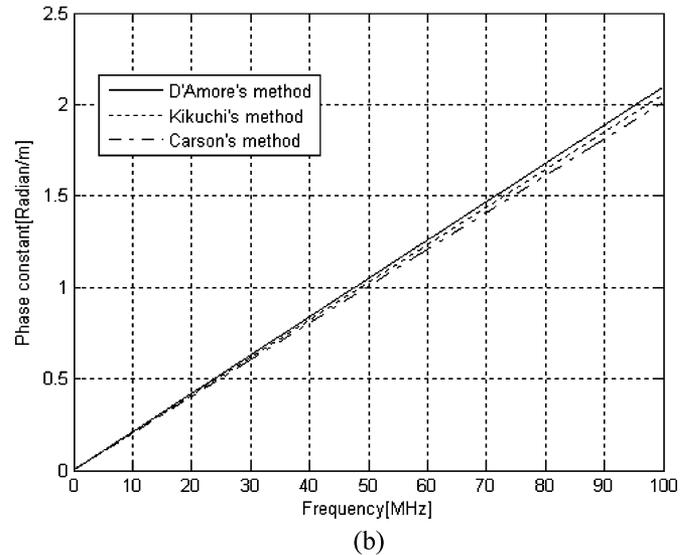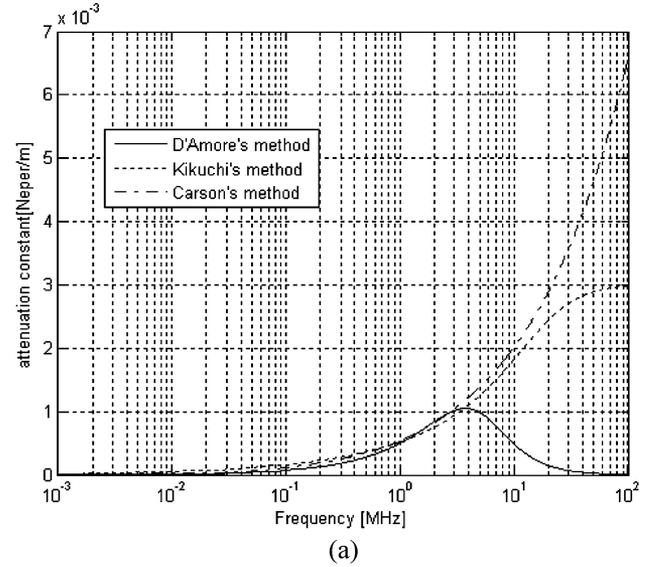

Fig. 1. (a) Real and (b) Imaginary parts of propagation constant of an overhead wire at a height of 10 m above ground, obtained by three different methods.

but beyond a certain frequency, D'Amore's expression shows a decrease in the attenuation constant, Kikuchi's expression approaches a saturated level and Carson's result increases monotonically with frequency. The experimental measurements in [12], [19], and [16] are in agreement more with D'Amore's method rather than with the other two methods.

B. Analysis of Multiconductor Transmission Lines

Analysis of transmission lines consisting of two parallel conductors is a well-understood topic. This understanding can be further extended into matrix notations to cover multiconductor transmission lines (MTL), involving more than two conductors [20]. For a two-conductor line, we end up with forward- and reverse-traveling waves. For an MTL with $(n + 1)$ conductors placed parallel to the x axis, there are n forward- and n reverse-traveling waves with respective velocities. These waves can be described by a coupled set of $2n$, first-order matrix partial differential equations which relate the line voltages $V_i(x, t)$,
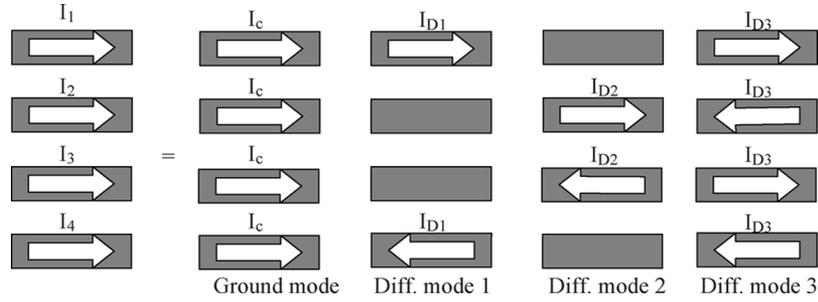
Fig. 2. Modes of four-wire power lines.

$i = 1, 2, \ldots, n$, and line currents $I_i(z, t)$, $i = 1, 2, \ldots n$. Each pair of forward- and reverse-traveling waves is referred to as a mode. For example, in a case involving four conductors and a ground return, we can define four modes, as shown in Fig. 2. Using these independent modes, we can decompose currents I_1 through I_4 as a linear combination of four modal currents. Common mode (also referred to as ground mode) is characterized by the highest attenuation among the modes, and is propagation through four phases and a return via ground. With signal propagation and return only through wires, differential modes (also known as the aerial modes) 1, 2, and 3 show a somewhat lower attenuation than the common mode.

In BoPL transmission, depending on the way signal is coupled onto the lines, either wire-to-wire (WTW) or wire-to-ground (WTG) injection is possible. For WTW injections, differential modes are mostly excited. For a WTG injection, in the case of coupling to the middle phase, common mode and differential modes are excited. Generally, these modes are not orthogonal unless the wavelength of electromagnetic wave inside the conductors is a small fraction of the height of the wires and the spacing between the wires is a small fraction of the wavelength [21]. This condition is satisfied for practical MV power line systems up to 100 MHz. Beyond this frequency, the discrete modes lose their orthogonality and continuous modes start to appear.

The prevalent mode of propagation in an MTL is TEM. An MTL is capable of guiding waves whose frequency values vary from DC to a point where the line cross-sectional dimensions such as line separations become a significant fraction of wavelength. At higher frequencies, higher order modes coexist with the TEM mode, so other guiding structures such as waveguides and antennas are more practical. Additionally, imperfections in the line conductors; presence of nearby conductors, and asymmetries in the physical terminal excitation such as offset source positions may also create non-TEM currents [20].

In a multiconductor geometry depicted in Fig. 3, n wires are placed in parallel with the x axis. Parameters h_i and a_i refer to the height above the earth and the radius of ith wire, respectively. Parameter Δ_{ij} is defined as the distance between the ith wire and the jth wire along the z axis. Distance parameter d_{ij} is defined as the shortest distance between the ith and the jth wires and can be described by

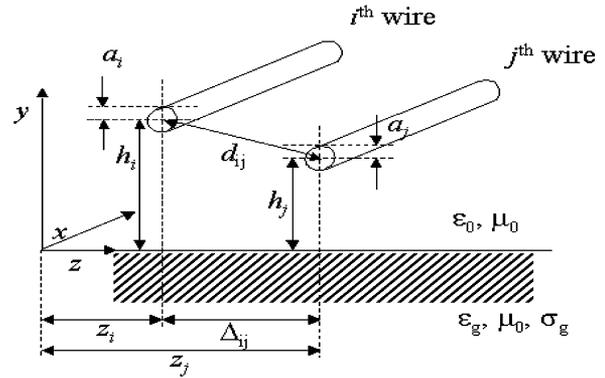$$d_{ij} = \sqrt{(h_i - h_j)^2 + \Delta_{ij}^2}. \tag{20}$$

Fig. 3. A multiconductor configuration.

Basically, this problem is analyzed by solving the so-called curl-Maxwell equations and satisfying the boundary conditions on each and every wire similar to the single conductor case. By doing so, the result for finding the transmission constant is the answer to matrix equations with Bessel and Sommerfeld integrals. The procedure is very similar to what we followed for a single wire, but it uses matrices instead of vectors.

Actually, taking a number of steps can solve for n line voltages and n line currents, describing an MTL. First, per-unit-length parameters such as inductance, capacitance, conductance, and resistance are determined for the considered line. Second, the MTL equations are solved in the form of a sum of n forward- and n reverse- traveling wave equations, with $2n$ unknown coefficients. Third, termination conditions such as independent voltage/current sources, load, and source impedance values are incorporated in the MTL equations in order to determine the $2n$ unknown coefficients [20].

As stated, the first step in solving the MTL equations is to obtain the per-unit-length parameters for the conductors. For this, Carson [13] suggested incorporating ground impedance. However, this model, without considering the ground admittance, is only suitable over low-frequency values and/or under good conductive ground plane conditions. Unfortunately, ground admittance does not have an explicit expression and it can be evaluated only by numerical methods. Therefore, as an effort to find a new ground return path model for higher frequencies and/or under poor ground conductivity conditions, a new procedure was suggested with some assumptions. This methodology by D'Amore et al. [12] incorporates the per-unit-length series-impedance and shunt-admittance matrices, using the curl-

Maxwell field equations. In this method, it is assumed that the wavelength of electromagnetic wave inside the conductors is a small fraction of the height of wires and the spacing between the wires is a small fraction of the wavelength. Therefore, the discrete modes are orthogonal. The details of this formulation are explained in the next section. Further physical justifications of these steps can be found in [12] and [19].

III. MATHEMATICAL DERIVATIONS

A. Multiconductor Configuration and Modal Analysis

The well-known second-order differential equations describing the propagation on a conductor can be extended to a matrix form as in (21), where $\mathbf{V}$ and $\mathbf{I}$ are n-by-1 column vectors of voltage and current in each wire, $\mathbf{P}$ is an n-by-n propagation matrix, and "t" represents the matrix transpose

$$\frac{d^2\mathbf{V}}{dx^2} = \mathbf{P}\mathbf{V}, \quad \frac{d^2\mathbf{I}}{dx^2} = \mathbf{P}^t\mathbf{I}. \tag{21}$$

Denoting the n-by-n *per-unit-length* series impedance matrix by $\mathbf{Z}$ and the n-by-n *per-unit-length* shunt-admittance matrix by $\mathbf{Y}$, the propagation matrix $\mathbf{P}$ can be expressed by

$$\mathbf{P} = \mathbf{Z}\mathbf{Y}. \tag{22}$$

Often, similarity transformation is adopted in the analysis of multiconductors, where a change in variables is defined, as in (23), such that the actual conductor voltage vector $\mathbf{V}$ and current vector $\mathbf{I}$ can be related to mode voltage vector $\mathbf{V}^m$ and mode current vector $\mathbf{I}^m$, as in [12]. The definitions of $\mathbf{M}$ and $\mathbf{N}$ are provided in [20] and [12]

$$\mathbf{V} = \mathbf{M}\mathbf{V}^m \quad \text{and} \quad \mathbf{I} = \mathbf{N}\mathbf{I}^m. \tag{23}$$

Using the propagation matrix, propagation constant of the ith mode, γ_i can be represented by (24), with α_i and β_i being the attenuation and phase constants of the ith mode, respectively

$$\gamma_i = \sqrt{\lambda_i} = \alpha_i + j\beta_i, \qquad i = 1\ldots n \tag{24}$$

where λ_i is the ith eigenvalue of the propagation matrix.

Then, the general equation for modal currents can be expressed by (25), where the vectors of undetermined constants still need to be determined. Modal voltages can be determined, likewise. Actual voltages and currents of phases can be determined by (23)

$$\begin{bmatrix} I_1^m \\ \vdots \\ I_n^m \end{bmatrix} = \begin{bmatrix} e^{-\gamma_1 x} & \cdots & 0 \\ \vdots & \ddots & \vdots \\ 0 & \cdots & e^{-\gamma_n x} \end{bmatrix} \begin{bmatrix} I_1^{m+} \\ \vdots \\ I_n^{m+} \end{bmatrix}$$
$$- \begin{bmatrix} e^{\gamma_1 x} & \cdots & 0 \\ \vdots & \ddots & \vdots \\ 0 & \cdots & e^{\gamma_n x} \end{bmatrix} \begin{bmatrix} I_1^{m-} \\ \vdots \\ I_n^{m-} \end{bmatrix}. \tag{25}$$

Characteristics impedance and admittance matrices can be defined by (26)

$$\mathbf{Z_c} = \mathbf{Y_c^{-1}} = \mathbf{Y}'^{-1}\mathbf{N}\gamma\mathbf{N}^{-1} = \mathbf{Z}'\mathbf{N}\gamma^{-1}\mathbf{N}^{-1}. \tag{26}$$

B. Propagation Matrix Derivation

With the derivations in Section III-A, one needs to further characterize $\mathbf{P}$. This can be done by enforcing the continuity condition of the x-component of the E-field at each air-wire interface [12]. Following the reference, $\mathbf{P}$ can be expressed by internal, external, and ground impedance and admittance, as is given by (27). Each of the impedance and admittance terms are represented by (28), (30), and (32)–(34), where the definitions in (29), (31), and (35)–(38) are used

$$\mathbf{P} = \left(\mathbf{Z}'_i + \mathbf{Z}'_e + \hat{\mathbf{Z}}'_g\right)\left(\mathbf{Y}'^{-1}_e + \hat{\mathbf{Y}}'^{-1}_g\right)^{-1} \tag{27}$$

$$\mathbf{Z}'_i = \text{diag}\left\{Z'_{i1}\ldots Z'_{ij}\ldots Z'_{in}\right\}$$

$$Z'_{ij} = \frac{\mu_w f \mathrm{I}_0(jk_w a_i)}{a_i k_w \mathrm{I}_1(jk_w a_i)} \tag{28}$$

I_0 first kind Bessel function of zeroth-order
I_1 first kind Bessel function of first-order

$$k_w = k_0\left(\frac{\varepsilon_w}{\varepsilon_0} - j\frac{\sigma_w}{\omega\varepsilon_0}\right)^{1/2}, \text{ where : } k_0 = \omega\sqrt{\mu_0\varepsilon_0} \tag{29}$$

$$\mathbf{Z}'_e = \frac{j\omega\mu_0}{2\pi}\mathbf{A} \tag{30}$$

A is a matrix corresponding to the characteristics of each wire and the relation to those of other wires, with elements equal to

$$A_{ii} = \ln\frac{2h_i}{a_i}, \; A_{ij} = \ln\frac{D_{ij}}{d_{ij}},$$
$$D_{ij} = \left[(h_i + h_j)^2 + \Delta_{ij}^2\right]^{1/2} \tag{31}$$
$$\mathbf{Y}'_e = j\omega\varepsilon_0 2\pi\mathbf{A}^{-1} \tag{32}$$
$$\hat{\mathbf{Z}}'_g = \frac{j\omega\mu_0}{\pi}\mathbf{F}_{1g} \tag{33}$$
$$\hat{\mathbf{Y}}'_g = j\omega\varepsilon_0\pi\mathbf{F}_{2g}^{-1} \tag{34}$$

F_{1g} and F_{2g} are matrices representing the characteristics of each wire with respect to the ground and to other wires, with elements equal to:

$$F_{1gij} = \frac{1}{2}\ln\frac{h_i + h_j + j\Delta_{ij} + \xi_1}{h_i + h_j + j\Delta_{ij}} \tag{35}$$

$$F_{2gij} = \xi_2\ln\frac{h_i + h_j + j\Delta_{ij} + \xi_3}{h_i + h_j + j\Delta_{ij}} \tag{36}$$

$$\xi_1 = \frac{2}{\sqrt{k_0^2 - k_g^2}}, \; \xi_2 = \frac{k_0^2}{k_0^2 + k_g^2},$$

$$\xi_3 = \frac{k_0^2 + k_g^2}{k_0^2\sqrt{k_0^2 - k_g^2}} \tag{37}$$

$$k_g = k_0\sqrt{\frac{\varepsilon_g}{\varepsilon_0} - j\frac{\sigma_g}{\omega\varepsilon_0}}. \tag{38}$$

C. Per-Unit-Length Series Impedance and Shunt-Admittance Matrices Derivations

Derivations in Section III-B can be used to obtain the propagation matrix. However, to derive $\mathbf{Z}$ and $\mathbf{Y}$, more rigorous expressions should be applied for several reasons outlined in [12]. Therefore, one needs to evaluate $\mathbf{Z}'_g$ in (39) by evaluating $\mathbf{P^t}$ from (27) and $\mathbf{F}_{3g}$ in (40). $\mathbf{Z}'_g$ can then be used in (41) in order to obtain $\mathbf{Z}$. Also, $\mathbf{Y}'_g$ can be calculated by (42), yielding (43). This process is necessary in order to calculate the exact value of the per-unit-length series impedance and shunt admittance matrices

$$\mathbf{Z}'_g = \frac{j\omega\mu_0}{\pi}\mathbf{F}_{1g} - \frac{1}{j\omega\varepsilon_0\pi}\mathbf{F}_{3g}\mathbf{P}^t \tag{39}$$

$$F_{3gij} = \xi_2 \ln \frac{h_i + j\Delta_{ij} + \xi_3}{h_i + j\Delta_{ij}} \tag{40}$$

$$\mathbf{Z} = \mathbf{Z}'_i + \mathbf{Z}'_g + \mathbf{Z}'_e \tag{41}$$

$$\mathbf{Y}'_g = j\omega\varepsilon_0\pi(\mathbf{F}_{2g} - \mathbf{F}_{3g})^{-1} \tag{42}$$

$$\mathbf{Y} = j\omega\varepsilon_0\pi\left(\frac{1}{2}\mathbf{A} + \mathbf{F}_{2g} - \mathbf{F}_{3g}\right)^{-1}. \tag{43}$$

IV. BoPL Network Channel Model and Capacity

Frequency response, H(f), of a matched transmission line can be expressed by means of a propagation constant γ. In [23], voltage along the conductor at a distance l from the source $V(l)$, is obtained by

$$V(l) = H(f)V(0) \tag{44}$$

$$H(f) = e^{-\gamma(f)l} = e^{-\alpha(f)l}e^{-j\beta(f)l} \tag{45}$$

where $V(0)$ is the voltage at the source. By having the propagation constant, one may easily find a transfer function for power line wire at a desired point on the conductor. As discussed later, each mode of coupling has a different propagation constant. Hence, there is a different frequency response for each mode.

Part of a propagating signal reflects back to the transmitter at branch junctions due to impedance mismatch and the remainder travels through [23]. Reflection coefficient is defined for each node as the ratio of the reflected signal power to the total received signal power at the node. In the same way, transmission coefficient is defined as the ratio of the transferred signal power to the total received signal power at the node. Obviously, reflection and transmission coefficients are equal or less than unity and the sum of all transmission and reflection coefficients at each node is unity.

Reflections cause signal propagation not to take place along a single straight path from a transmitter to a receiver in a power line network. Additional paths may also exist due to reflections at the network junctions. This creates a multipath channel with frequency selectivity, similar to that in a wideband radio channel. As such, a transfer function for linear systems with memory can be used to characterize these lines. When signal passes through a junction, it will be multiplied by transmission coefficient of the junction and when it reflects back from a junction, it will be weighted by reflection coefficient of that junction.
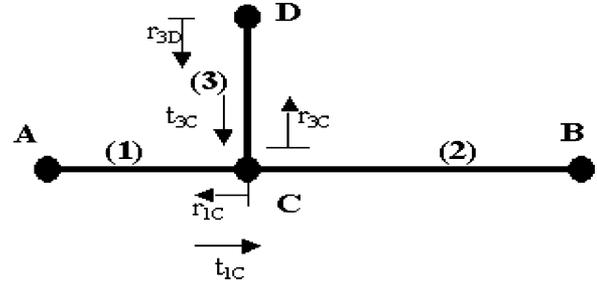

Fig. 4. Multipath signal propagation; cable with a single tap.

Therefore, each arrived path at a receiver is weighted by a factor g, which is the product of reflection and transmission coefficients of nodes along the path. As reflection and transmission coefficients are equal or less than one, the weighting factors are equal or less than unity, as well [24].

For better explanation, multipath signal propagation can be studied by a simple example, which can be easily analyzed in Fig. 4. The link has only one branch and consists of the segments (1)–(3) with lengths l_1, l_2, l_3, and the impedance values $\mathbf{Z}_{l1}$, $\mathbf{Z}_{l2}$, and $\mathbf{Z}_{l3}$ that are equal to the product *per-unit-length* impedance of each branch by its length.

In order to simplify the considerations, $\boldsymbol{A}$ and $\boldsymbol{B}$ are assumed to be matched, which means $\boldsymbol{Z_A} = \boldsymbol{Z_{l1}}$ and $\boldsymbol{Z_B} = \boldsymbol{Z_{l2}}$. The remaining points for reflections are $\boldsymbol{C}$ and $\boldsymbol{D}$, with the reflection factors denoted as $\boldsymbol{r_{1C}}$, $\boldsymbol{r_{3C}}$, $\boldsymbol{r_{3D}}$, and the transmission factors denoted as $\boldsymbol{t_{1C}}$, $\boldsymbol{t_{3C}}$. These values are given by

$$r_{1c} = \frac{(Z_{l2}\|Z_{l3}) - Z_{l1}}{(Z_{l2}\|Z_{l3}) + Z_{l1}} \tag{46}$$

$$r_{3D} = \frac{Z_D - Z_{l3}}{Z_D + Z_{l3}} \tag{47}$$

$$r_{3c} = \frac{(Z_{l2}\|Z_{l1}) - Z_{l3}}{(Z_{l2}\|Z_{l1}) + Z_{l3}} \tag{48}$$

$$t_{1c} = 1 - |r_{1c}| \tag{49}$$

$$t_{3c} = 1 - |r_{3c}|. \tag{50}$$

These equations can be extended to a matrix form for a multiwire scenario. With these assumptions, in principle, an infinite number of propagation paths is possible due to multiple reflections (i.e., $A \rightarrow C \rightarrow B$, $A \rightarrow C \rightarrow D \rightarrow C \rightarrow B$, $A \rightarrow C \rightarrow D \rightarrow C \rightarrow D \rightarrow C \rightarrow B$, and so on). Each path $\boldsymbol{i}$ has a weighting factor, $\boldsymbol{g_i}$, representing the product of the reflection and transmission factors along the path. The more transitions and reflections occur along a path, the smaller the weighting factor will be, because, as mentioned earlier, transmission and reflection coefficients are less than one. Furthermore, longer paths exhibit higher attenuation, so that they contribute less to the overall signal at the receiving point. Due to these facts, it is reasonable to approximate the basically infinite number of paths by finite number of dominant paths.

With these weighting coefficients, we may express the network as a summation of multiple paths with different length and weighting factors. The propagation along a wire follows (44), so

one can easily express the multipath network channel model [4], [7] and [24] as

$$H(f) = \sum_{i=1}^{N} g_i e^{-\alpha(f)d_i} e^{-j\beta(f)d_i} \tag{51}$$

where N is the number of significant arrived paths at the receiver, d_i is the length of the ith path, and g_i is the weighting factor of the ith path. This expression is the transfer characteristics of all cables; however, it uses a propagation constant that is appropriate for overhead MV power lines.

Now, that the frequency response has been defined, by identifying the noise spectral density, water-filling [25] in spectral domain can be applied to express the channel capacity as

$$c = \int_{-\infty}^{\infty} \frac{1}{2} \log_2 \left[1 + \frac{\left(p - \frac{N_0(f)}{2|H(f)|^2} \right)^+}{\frac{N_0(f)}{2|H(f)|^2}} \right] df \tag{52}$$

where p is the signal power at the specific frequency and is chosen such that $\int_{-\infty}^{\infty} (p - (N_0(f)/2|H(f)|^2))^+ df = P$. The notation $[X]^+$ means Max $\{X, 0\}$ and P is the average transmitted power. In (52), $N_0(F)$ is the noise spectral density in the system.

Over MV lines, two types of noise are dominant: colored background noise and narrowband noise [9]. The former is the environmental noise, which is highly dependant on the weather, geography, above ground height, etc. Corona discharge is a major cause of background noise, especially under humid and severe weather conditions [26]. When MV power line is in operation, a strong electric field exists in the vicinity of wires. This field accelerates free electron charges in the air surrounding the conductors. These electrons interact with the molecules in the air and produce free electrons and positive ions. This process causes an avalanche, called corona discharge. The discharge induces current pulses in conductors with random variations of amplitude and separation time. Induced currents can be modeled with current sources in power line system.

Narrowband noise is the interference from other narrowband wireless devices and services in the frequency range of BoPL systems, like amateur or shortwave radios. Narrowband noise differs from time to time and place to place because the BoPL frequency range is not occupied in all places by radio signals, uniformly. Also, narrowband noise is time dependent.

V. NUMERICAL COMPUTATION RESULTS AND DISCUSSION

For numerical computation purpose, we used a four-wire configuration with a 10 m height above ground and 70 cm spacing between wires; each wire assumed to have 2 cm diameter. The ground plane, on an average base, is characterized by a relative permittivity of $\varepsilon_g = 13$ and conductivity of $\sigma_g = 5$ S/m.

The frequency spectra of four propagation constants are computed by using the method described earlier and the attenuation constants are shown in Fig. 5.
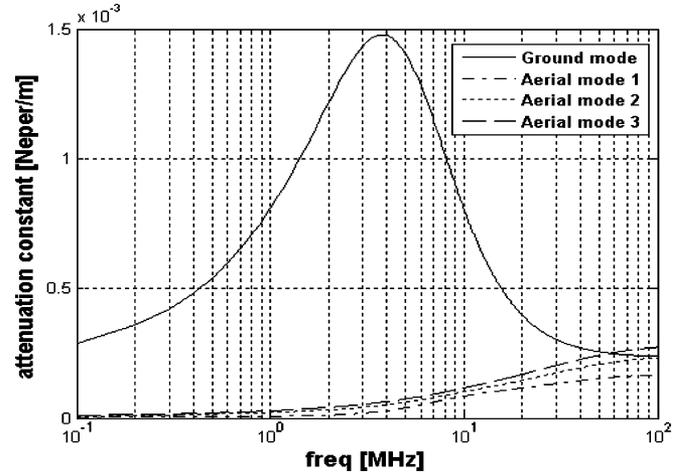

Fig. 5.   Frequency spectra of attenuation constants of an MTL system.

The attenuation constants of each mode exhibit a different behavior and values. Common mode shows higher attenuation over the frequency range and the attenuation factors for the three aerial modes are close to one another. Common mode attenuation factor increases up to some frequency and decays beyond. This incident is due to resonance phenomenon in ground medium, initially capacitive and by increasing frequency it exhibits an inductive behavior. This can be observed in Fig. 6 that illustrates real and imaginary parts of characteristic impedance of a line with common mode injection. The real part of characteristic impedance is always characterized by positive values, because the line is a passive system. At low frequencies, the displacement currents are insignificant and ground plane acts as a good conductor. Therefore, the proper terms of the input impedance matrix of the line are capacitive and the imaginary part of the characteristic impedance shows negative values. On the contrary, at higher frequencies ground can be considered as a good dielectric and the proper terms of the input equivalent impedance matrix become inductive. This makes the imaginary part of the characteristic impedance positive. The null value is reached at the resonance frequency, corresponding to the minimum of the real part.

Fig. 7(a) represents frequency response of a matched transmission channel over a 1 km span MTL system. As the system is matched, signal does not get reflected at the receiver-end and signal path is a straight point-to-point path. In this case, the only loss comes from MTL path loss. Fig. 7(a) depicts frequency response for two coupling methods: common mode and differential mode 1. Common mode exhibits more loss than differential mode, especially at low frequencies. As frequency increases, losses of the two configurations become comparable. Also, one may notice that both systems show a very low loss at high frequencies over a 1 km repeater span. The fact that MV overhead power lines resemble a low loss transmission system shows promise for data delivery at high rates. Also, this is a cause for concern, regarding potential interference into existing services, as elaborated on extensively in NTIA reports [11]. Interference problem must be remedied, as stated earlier. The root cause of
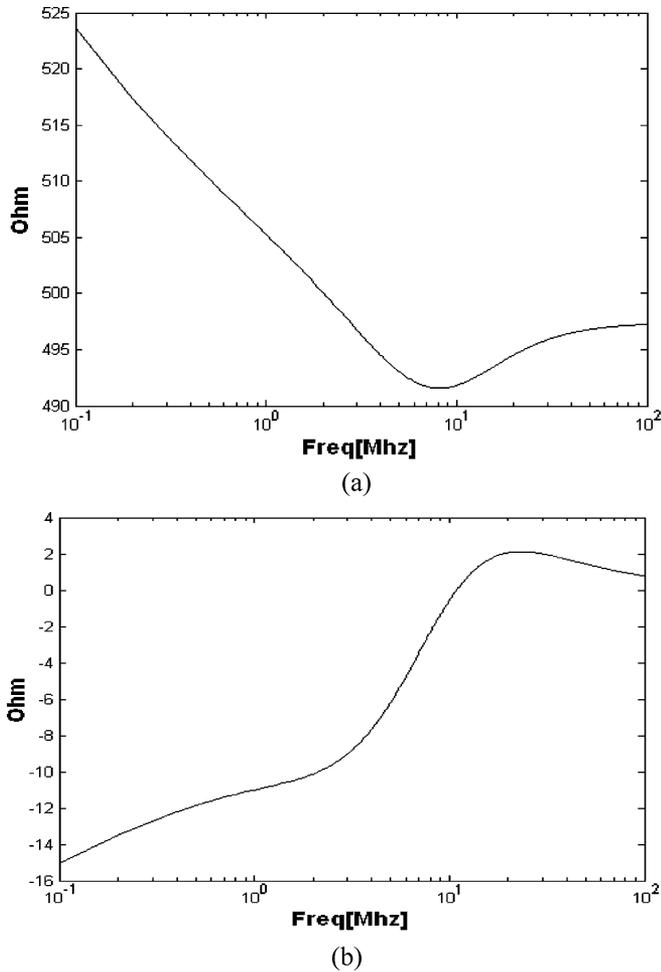
(a)

(b)

Fig. 6. Frequency spectra of (a) real and (b) imaginary parts of characteristic impedance of a multiconductor line with common mode injection.
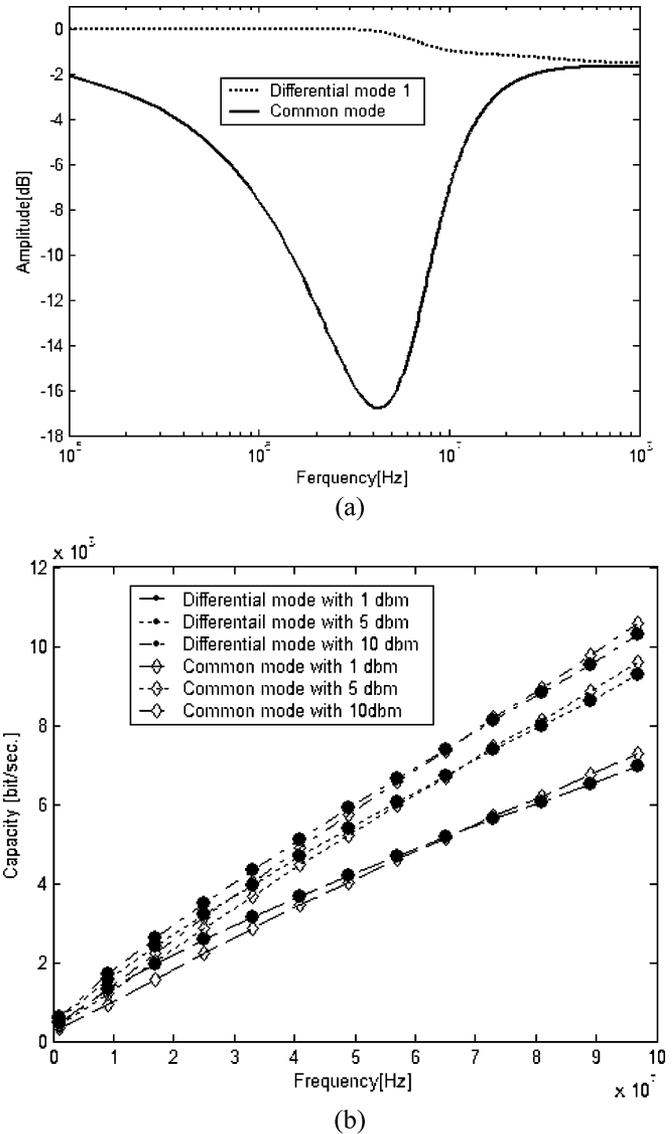

(a)

(b)

Fig. 7. (a) Frequency response of matched MTL transmission over 1 Km for differential and common mode coupling. (b) Corresponding capacity values for different coupling methods and transmit power levels.
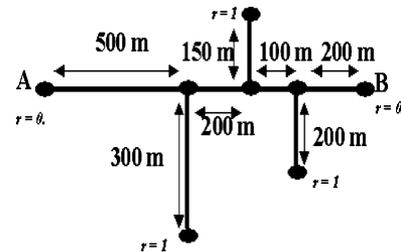

Fig. 8. Simulated complex network.

interference can be found in discontinuities and asymmetrical MTL loads.

Channel capacity is the maximum transmission rate over a channel, regardless of modulation or any other systems considerations. It depends on the channel characteristics. As we know, the interference and narrowband noise vary from place-to-place and time-to-time and there is no known model for these. As yet, no significant measurement results are available. However, these obstacles can be overcome by proper countermeasure techniques. Therefore, as the definition of channel capacity suggests, one should only consider the nonresolvable limitations of a channel that are common in all power grids. The additive background noise in BoPL is the only consistent noise in this system. Therefore, it is sensible to use the PSD of this noise to calculate the capacity limit of MV power line grid. Fig. 7(b) illustrates the water-filling channel capacity limits of (52) for a matched transmission system with a 1 Km repeater span at different transmitted power levels. For evaluating channel capacity, we chose a uniform -105 dBm/Hz spectral level as a representative of average noise spectral density height of background noise. Referring to [9], this value is a conservative average estimate of practical background noise level for MV power lines. Also, compared with galactic noise model, the

assumption on noise level seems reasonable. It is interesting to see both differential and common modes coupling systems show almost the same average capacity characteristics, especially at high frequencies. This is due the fact that both systems approach the same loss level at higher frequencies.

According to Fig. 7(b), with an ideal matched MTL system, over 50 MHz of channel band, we can deliver almost 600 Mb/s
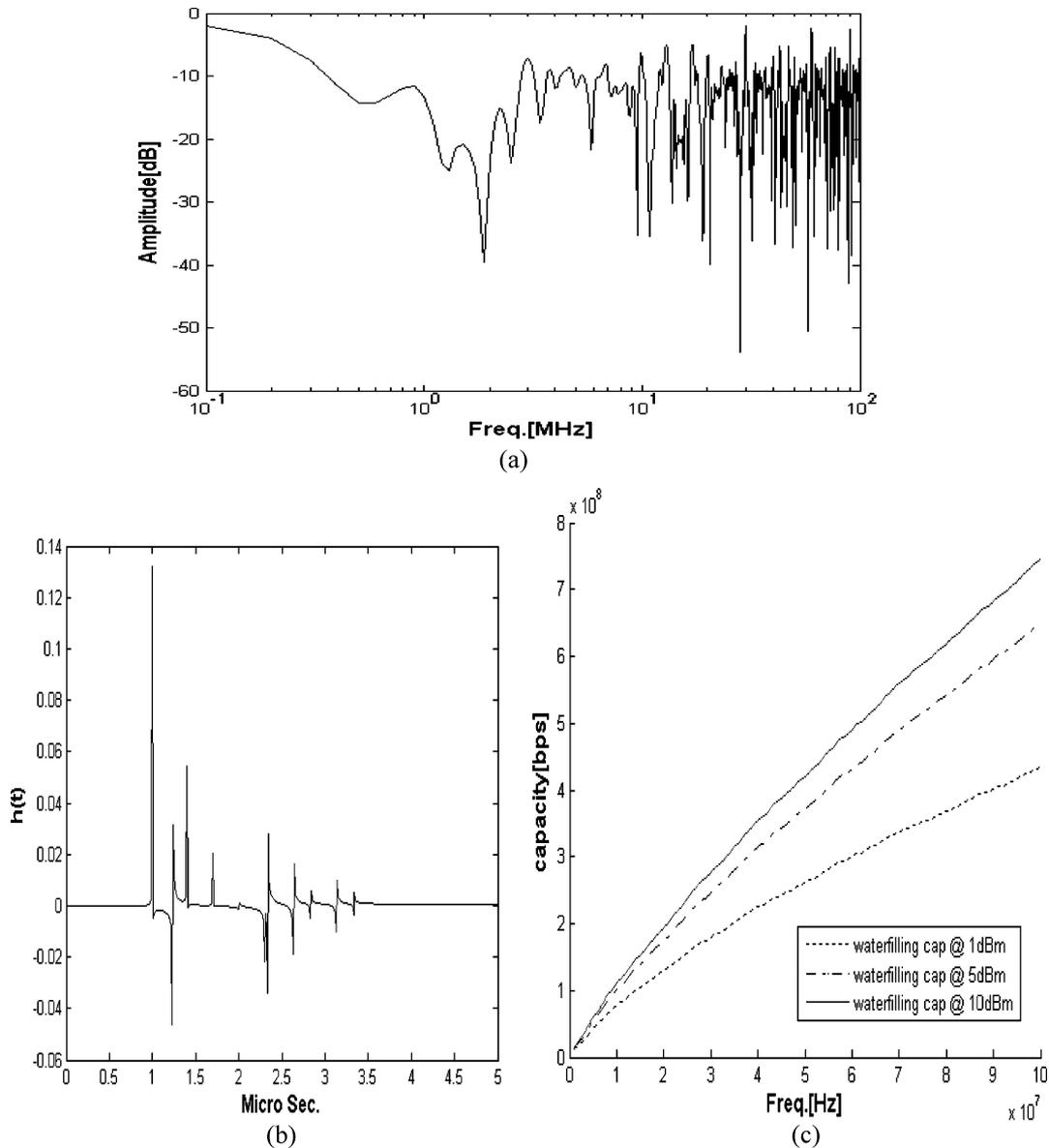
Fig. 9.   (a) Amplitude of frequency response of complex network shown in Fig. 8 using D'Amore's formulation for propagation constant and (b) its impulse response, and (c) line's transmission capacity bounds.

by launching 10 dBm transmit power. In reality, this low loss nature of MTL systems degrades as a result of several impairments. As stated earlier, mismatch at junctions cause traveling signal to get reflected back, creating multipath. This can decrease the average channel capacity value.

Over an actual power line network, there always exist several branches and junctions between a transmitter and a receiver. These branches cause nulls in transmission channel frequency response due to multipath. To investigate this phenomenon, we simulated the complex network shown in Fig. 8. In this network, we have three branches between transmitter and receiver. Each end of these branches is an open circuit, so reflection factor at each end is assumed unity. Also, we have assumed that transmitter or receiver impedance is matched to that of the line. Impedance of each branch is related to length of that branch and according to those impedance values, each junction has an associated reflection and transmission coefficient.

Our simulation program performs an exhaustive search for all possible paths from the transmitter to the receiver and eliminates those paths that have a power less than 1% of straight path power. Fig. 9(a) shows the complex grid magnitude of frequency responses. Reflections create deep nulls in the frequency response. Simulation shows there are 11 dominant paths and from Fig. 9(b), 11 pulses with different arrival times are distinguished. Delay spread in this network is almost 3 μs. Fig. 9(c) is the illustration of the channel capacity limits for this complex network. The average capacity in this network with a 10 dBm launched transmit power level at 50 MHz band is about 400 Mb/s. Obviously, the junctions and branches between transmitter and receiver degrade the system performance extensively compared with the ideal point-to-point case.

The same modeling program is used for our sample complex network with Carson's formulation for propagation constant [13] and the results are depicted in Fig. 10. It is seen from
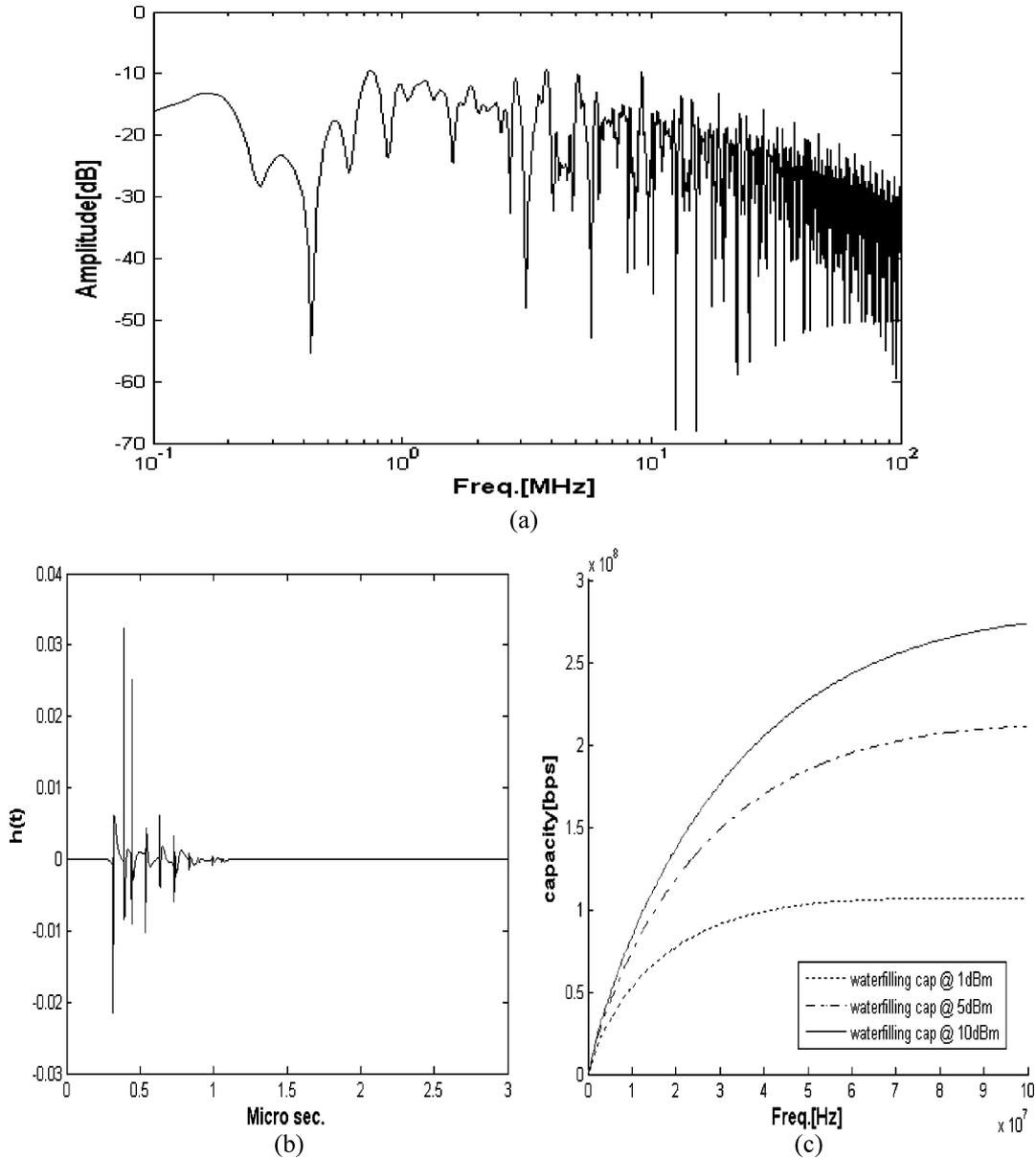
Fig. 10. (a) Amplitude of frequency response of complex network shown in Fig. 8 using Carson's formulation for propagation constant and (b) its impulse response, and (c) line's transmission capacity bounds.

Fig. 10(a) that the Carson's model shows more loss than the D'Amore's method. However, the delay spread is decreased to 1 μs, as it is shown in Fig. 10(b). Due to the high loss of the channel, there are less significant signal paths from the transmitter to the receiver. Although the delay spread of this model is lower than the D'Amore's model, the channel capacity limits of this model in Fig. 10(c) is significantly decreased compared with the values in Fig. 9(c). By using Carson's formulation, the predicted capacity at 50 MHz is close to 250 Mb/s, whereas it is 400 Mb/s using D'Amore's method. Thus, using Carson's model, potential of OH power lines is underestimated as the omnipresent means for broadband communications.

Having stated all the salient features, in a real power line grid, it must be remembered that in most North American urban and suburban areas the electricity distribution poles do not only carry MV electricity distribution cables, but they also carry street lighting, telecom, and CATV cables, which are generally located some (safe) distance below the MV/LV distribution conductors. HF propagation models must therefore incorporate these metallic elements if the modeling results are to be validated in practice. Also, one must consider the effects of relatively large pole-mounted capacitor banks and the MV/LV transformers. Also, in North America, many utilities provide neutral grounding and/or grounding of the wooden support poles and/or grounding of surge-diverters (i.e., tip-to-toe, to protect the poles and/or insulators in the event of lightning strikes and resulting voltage surges), if this is not accounted for in the modeling then, once again, the predictions may well be over optimistic.

Another key issue on MV lines occurs at some road crossings, subways, underpasses, and some lateral sections which, of necessity, require underground cable sections to be deployed. At

such points, the relatively high impedance OH open wires are terminated in relatively low impedance underground cable sections and, as a result, the high-frequency communication signals suffer severe attenuation. So, once again, care must be taken not to generalize, and therefore raise expectations, which may not be achievable in practice.

Another very important factor that should be considered for evaluating BoPL system performance is interference to other wireless systems or electromagnetic compatibility (EMC) issues [28], [29]. As stated earlier, the NTIA reports [11] on potential for interference in using BoPL are excellent sources to consider in this regard.

VI. CONCLUSION

This research examined the potential of MV overhead power lines as a communications medium for broadband transmissions. Available models for overhead power lines were not suitable for high frequencies with lossy ground return. D'Amore *et al.* in [12] proposed a model for multiwires over ground, which is more suitable for application of BoPL systems using overhead MV lines. Based on this model, we developed a new channel transfer characteristic function model. Our simulations show ideal overhead power lines exhibit a low loss with a capacity limit of about 1 Gb/s over a 1 Km repeater span; if 10 dBm transmit power and 100 MHz of channel bandwidth are available. Junctions and branches in power line network cause signals to bounce back and produce a multipath channel. This causes degradation in power line system performance and decreases channel capacity. Removing discontinuities by adaptive impedance matching [27] on these lines can potentially enhance the lines data handling capacity. For a sample grid, comparison was made to the capacity value predicted based on the Carson's model and it is demonstrated that the older model underestimates the potential of the overhead lines for broadband transmissions, largely.

REFERENCES

[1] P. Amirshahi and M. Kavehrad, "Transmission channel model and capacity of overhead multi-conductor medium-voltage power-lines for broadband communications," in *Proc. CCNC*, Las Vegas, NV, Jan. 2005, pp. 354–358.

[2] J. Dickinson and P. Nicholson, "Calculating the high frequency transmission line parameters of power cables," in *Proc. Int. Symp. Power Line Commun. Appl.*, 1997, pp. 127–133, 2nd ed.

[3] K. Dostert, "RF-models of the electrical power distribution grid," in *Proc. 1998 Int. Symp. Power Line Commun. Appl.*, 1998, pp. 105–114.

[4] H. Philipps, "Modeling of powerline communication channels," in *Proc. Int. Symp. Power Line Commun. Appl.*, 2000, pp. 14–25.

[5] T. Esmailian, F. R. Kschischang, and P. G. Gulak, "Characteristics of in-building power lines at high frequencies and their channel capacity," in *Proc. 2000 Int. Symp. Power Line Commun. Appl.*, 2000, pp. 52–59.

[6] F. J. Cañete, L. Díez, and J. T. Entrambasaguas, "Indoor power-line communications: Channel modeling and measurements," in *Proc. Int. Symp. Power Line Commun. Appl.*, 2000, pp. 117–122.

[7] H. Philipps, "Development of a statistical model for power-line communication channels," in *Proc. Int. Symp. Power Line Commun. Appl.*, 2000, pp. 153–160.

[8] E. Yavuz, F. Kural, N. Coban, B. Ercan, and M. Safak , "Modeling of power-lines for digital communications," in *Proc. Int. Symp. Power Line Commun. Appl.*, 2000, pp. 161–168.

[9] J.-J. Lee, S.-J. Choi, H.-M. Oh, W.-T. Lee, K.-H. Kim, and D.-Y. Lee, "Measurements of the communications environment in medium voltage power distribution lines for wide-band power line communications," in *Proc. Int. Symp. Power Line Commun. Appl.*, 2004, pp. 69–74.

[10] H.-M. Oh, J.-J. Lee, K.-H. Kim, and K.-C. Whang, "Wideband channel impulse response measurement method using PN sequences for the medium voltage power distribution line channel," in *Proc. Int. Symp. Power Line Commun. Appl.*, 2004, pp. 74–78.

[11] NTIA, Potential interference from broadband over power line (BPL) systems to federal government radio communications at 1.7–80 MHz Phase 1 Study Vol. 1, NTIA Rep. 04-413, Apr. 2004. [Online]. Available: http://www.ntia.doc.gov/ntiahome/fccfilings/2004/bpl/FinalReportAdobe/VolumeI/COVERVOL1.pdf.

[12] M. D'Amore and M. S. Sarto, "A new formulation of lossy ground return parameters for transient analysis of multi-conductor dissipative lines," *IEEE Trans. Power Del.*, vol. 12, no. 1, pp. 303–314, Jan. 1997.

[13] J. R. Carson, "Wave propagation in overhead wires with ground return," *Bell Syst. Tech. J.*, vol. 5, pp. 539–554, 1926.

[14] H. Kikuchi, "Wave propagation along an infinite wire above ground at high frequencies," *Proc. Electrotech. J.*, vol. 2, pp. 73–78, Dec. 1956.

[15] ——, "On the transition form a ground return circuit to a surface waveguide," in *Proc. Int. Congr. Ultrahigh Frequency Circuits Antennas*, Paris, France, Oct. 1957, pp. 39–45.

[16] J. R. Wait, "Theory of wave propagation along a thin wire parallel to an interface," *Radio Sci.*, vol. 7, pp. 675–679, Jun. 1972.

[17] J. R. Wait and D. A. Hill, "Propagation along a braided coaxial cable in a circular tunnel," *IEEE Trans. Microw. Theory Tech.*, vol. 23, pp. 401–405, May 1975.

[18] R. G. Olsen, E. F. Kuester, and D. C. Chang, "Modal theory of long horizontal wire structures above the earth—Part II: Modes," *Radio Sci.*, vol. 13, pp. 615–623, Jul.–Aug. 1978.

[19] M. D'Amore and M. S. Sarto, "Simulation models of a dissipative transmission line above lossy ground for a wide-frequency range-Part I: Single conductor configuration," *IEEE Trans. Electromagn. Compat.*, vol. 38, no. 2, pp. 127–138, May 1996.

[20] R. P. Clayton, *Analysis of Multi-Conductor Transmission Lines*. New York: Wiley, 1994.

[21] R. G. Olsen and M. D. Wu, "High Frequency propagation losses on an open wire transmission line above dissipative earth," *IEEE Trans. Broadcast.*, vol. 34, no. 2, pp. 292–300, Jun. 1988.

[22] D. C. Chang and R. G. Olsen, "Excitation of an infinite wire above dissipative earth," *Radio Sci.*, vol. 10, no. 8–9, pp. 823–831, Aug.–Sep. 1975.

[23] D. K. Cheng, *Fundamentals of Engineering Electromagnetic*. New York: Addison-Wesley, 1992.

[24] M. Zimmerman and K. Dostert, "A multipath model for the power-line channel," *IEEE Trans. Commun.*, vol. 50, no. 4, pp. 553–559, Apr. 2002.

[25] T. M. Cover and A. T. Joy, *Elements of Information Theory*. New York: Wiley, 1991.

[26] CIGRE study Committee 35 Sep. 2000, Report on digital powerline carrier.

[27] P. C. Romero, "ADAPT: An automatic impedance adapter for medium-voltage communications equipment," in *Proc. Int. Symp. Power Line Commun. Appl.*, 2000, pp. 218–224.

[28] P. Amirshahi and M. Kavehrad, "Medium voltage overhead power-line broadband communications; transmission capacity and electromagnetic interference," in *Proc. Int. Symp. Power Line Commun. Appl.*, Vancouver, BC, Canada, Apr. 2005, pp. 2–6.

[29] P. S. Henry, "Interference characteristics of broadband power line communication systems using aerial medium voltage wires," *IEEE Commun. Mag.*, pp. 92–98, Apr. 2005.

[30] M. E. Hardy, S. Ardalan, and J. B. O'Neal, "A model for communication signal propagation on three phase power distribution lines," *IEEE Trans. Power Del.*, vol. 6, no. 3, pp. 966–972, Jul. 1991.

[31] S. Galli and T. Banwell, "A novel approach to the modeling of the indoor power line channel—Part II: Transfer function and its properties," *IEEE Trans. Power Del.*, vol. 20, no. 3, pp. 1869–1879, Jul. 2005.

Pouyan Amirshahi (S'02) was born in Santa Monica, CA, in 1979. He received the B.Sc. degree in electrical engineering from the Sharif University of Technology, Tehran, Iran, in 2002. He is currently working towards the Ph.D. degree at the Department of Electrical Engineering, Center for Information and Communications Technology Research (CICTR), Pennsylvania State University, University Park.

He is a member of the IEEE Broadband Over Power Lines Communications Subcommittee. His research interests span over wireless communications, networking, channel coding, and power line communications.

Mohsen Kavehrad (F'92) received the Ph.D. degree in electrical engineering from the Polytechnic University (Brooklyn Polytechnic), Brooklyn, NY, in 1977.

From 1978 to 1989, he worked on telecommunications problems for Fairchild Industries, GTE (Satellite and Laboratories), and AT&T Bell Laboratories. In 1989, he joined the Department of Electrical Engineering, University of Ottawa, Ottawa, ON, Canada, as a Full Professor. Since January 1997, he has been with the Department of Electrical Engineering, Pennsylvania State University, as W. L. Weiss Chair Professor and the Founding Director of the Center for Information and Communications Technology Research. During 1997–1998, he was also the CTO and a Vice President at Tele-Beam, Inc., State College, PA. He spent a six-month sabbatical term as an Academic Visitor (Senior Technical Consultant) at AT&T Shannon Research Laboratories, Florham Park, NJ, in 2004. He has over 300 published papers, several book chapters, books, and patents in wireless systems and optical networks. His current research interests are in the areas of technologies, systems, and network architectures that enable the vision of the information age; e.g., Broadband-Wireless Communications Networked Systems and Optical Communications Networked Systems.

Dr. Kavehrad received three Bell Laboratory Awards for his contributions to wireless communications, the 1991 TRIO Feedback Award for a patent on an optical interconnect, the 2001 IEEE VTS Neal Shepherd Best Paper Award, three IEEE Lasers and Electro-Optics Society Best Paper Awards between 1991 and 1995, and a Canada NSERC Ph.D. Dissertation Award in 1995, with his graduate students. He is a former Technical Editor for the IEEE TRANSACTIONS ON COMMUNICATIONS, *IEEE Communications Magazine*, and the *IEEE Magazine of Lightwave Telecommunications Systems*. Presently, he is on the Editorial Board of the *International Journal of Wireless Information Networks*. He served as the General Chair of leading IEEE conferences and workshops. He has chaired, organized, and been on the advisory committee for several international conferences and workshops.